



HAL
open science

Generalized signal-dependent noise model and parameter estimation for natural images

Thanh Hai Thai, Florent Reiraint, Rémi Cogranne

► **To cite this version:**

Thanh Hai Thai, Florent Reiraint, Rémi Cogranne. Generalized signal-dependent noise model and parameter estimation for natural images. *Signal Processing*, 2015, 114, pp.164-170. 10.1016/j.sigpro.2015.02.020 . hal-01915653

HAL Id: hal-01915653

<https://hal.science/hal-01915653v1>

Submitted on 19 Mar 2019

HAL is a multi-disciplinary open access archive for the deposit and dissemination of scientific research documents, whether they are published or not. The documents may come from teaching and research institutions in France or abroad, or from public or private research centers.

L'archive ouverte pluridisciplinaire **HAL**, est destinée au dépôt et à la diffusion de documents scientifiques de niveau recherche, publiés ou non, émanant des établissements d'enseignement et de recherche français ou étrangers, des laboratoires publics ou privés.

Generalized Signal-Dependent Noise Model and Parameter Estimation for Natural Images

Thanh Hai Thai, Florent Retraint and, Rémi Cogranne**

*ICD - LM2S - University of Technology of Troyes - UMR STMR CNRS
12, rue Marie Curie - CS 42060 - 10004 Troyes cedex - France*

Abstract

The goal of this paper is to propose a generalized signal-dependent noise model that is more appropriate to describe a natural image acquired by a digital camera than the conventional Additive White Gaussian Noise model widely used in image processing. This non-linear noise model takes into account effects in the image acquisition pipeline of a digital camera. In this paper, an algorithm for estimation of noise model parameters from a single image is designed. Then the proposed noise model is applied with the Local Linear Minimum Mean Square Error filter to design an efficient image denoising method.

Keywords: Signal-Dependent Noise Model, Noise Measurement, Noise Parameter Estimation, Denoising.

1. Introduction

Noise has been studied for decades in computer vision, image processing and statistical signal processing because of its impact in various applications such as image denoising, image segmentation or edge detection. To improve performance in those applications, it is important to identify noise characteristics. Noise models proposed in the literature can be roughly divided into two groups: signal-independent and signal-dependent. A typical model for the group of signal-independent noise is the Additive White Gaussian Noise (AWGN) that is widely used in image processing. However, this signal-independent AWGN model is not relevant due to the dominant contribution of the Poisson noise corrupting a natural image acquired by imaging device [1, 2]. While signal-independent noise models assume the stationarity of noise in the whole natural image, regardless original pixel intensity, signal-dependent noise models take into account the proportional dependence of noise variance on the original pixel intensity. Signal-dependent noise models include Poisson noise or film-grain noise [3], Poisson-Gaussian noise [4, 5], heteroscedastic noise model [2, 6], and non-linear noise model [7, 8]. The signal-dependent noise model gives the noise variance as a function of pixel's expectation. This function can be linear [4, 5, 2, 6] or non-linear [7, 8]. To identify noise characteristics

*Corresponding author.

**With the financial support from Champagne-Ardenne region, IDENT project.

Email address: remi.cogranne@utt.fr (Rémi Cogranne)

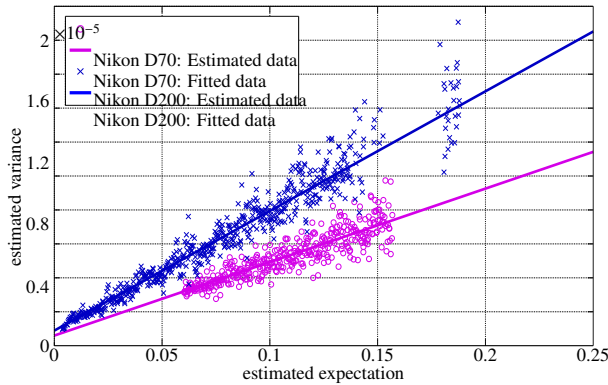


Figure 1: Scatter-plot of pixels' expectation and variance from RAW images acquired by *Nikon D70* and *Nikon D200* cameras [9].

or attenuate noise impact in many image processing applications, it is desirable to design an algorithm that estimates noise model parameters accurately.

Estimation of noise model parameters can be performed from a single image or multiple images. From a practical point of view, this paper mainly focuses on noise parameter estimation from a single image. Several methods have been proposed in the literature for estimation of signal-dependent noise parameters [2, 6, 7, 8]. They rely on similar basic steps but differ in details. The common methodology starts from obtaining local estimates of noise variance and image content, then performing the curve fitting to the scatter-plot based on the prior knowledge of noise model. The existing methods involve two main difficulties: influence of image content and spatial correlation of noise in a natural image. In fact, homogeneous regions where local means and variances are estimated are obtained by performing edge detection and image segmentation. However, the accuracy of those local estimates may be contaminated due to the presence of outliers (textures, details and edges) in the homogeneous regions. Moreover, because of the spatial correlation, the local estimates of noise variance can be overestimated. Overall, the two difficulties may result in inaccurate estimation of noise parameters.

The contribution of this paper is threefold. Firstly, by modeling the main steps of the image acquisition pipeline, this paper starts from the heteroscedastic noise model [2, 6] that accurately characterizes a natural RAW image and takes into account the impact of gamma correction to develop a generalized non-linear noise model. This model has not been proposed yet in the literature. Secondly, an algorithm for estimation of noise model parameters from a single image is proposed. Finally, the Local Linear Minimum Mean Square Error (LLMMSE) filter that was proposed in [3] is combined with the proposed noise model to design an efficient image denoising method.

The paper is organized as follows. Section 2 presents the generalized signal-dependent noise model for a natural image. Next, Section 3 designs the algorithm for estimation of noise model parameters. Section 4 presents numerical results on synthetic images and real natural images. Finally, Section 5 concludes the paper.

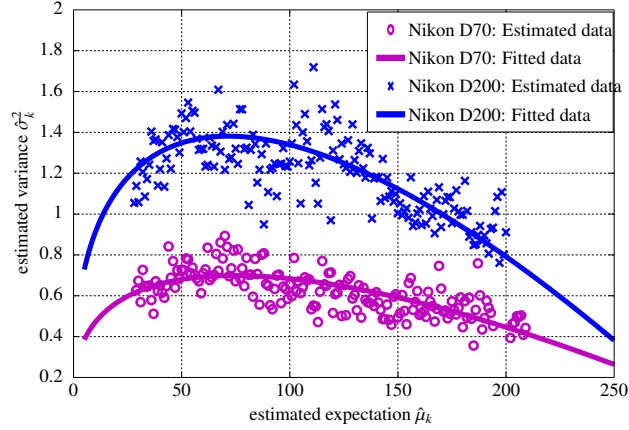


Figure 2: Scatter-plot of pixels' expectation and variance from JPEG images acquired by *Nikon D70* and *Nikon D200* cameras [9].

2. Generalized Signal-Dependent Noise Model

Image processing pipeline involves several steps from light capturing to image storage performed in a digital camera, see details about image processing pipeline in [10, 11, 12]. After measuring light intensity at each pixel, RAW image that contains exactly information recorded by the image sensor goes through some typical post-acquisition processes, e.g. demosaicing, white-balancing and gamma correction, to render a full-color high-quality output image, referred to as TIFF image.

RAW image can be modeled by considering noise sources that corrupt the image during its acquisition process [1, 2, 6]. Typically, the RAW image model consists of a Poissonian part that addresses the photon shot noise and dark current and a Gaussian part for the remaining stationary disturbances, e.g. read-out noise. For the sake of simplification, the Gaussian approximation of the Poisson distribution can be exploited because of a large number of incident photons, which leads the heteroscedastic noise model [6, 2]

$$x_i \sim \mathcal{N}(\mu_{x_i}, a\mu_{x_i} + b), \quad (1)$$

where x_i denotes a RAW pixel, $i \in \{1, \dots, N\}$ and N is the number of pixels. By convention, μ_X and σ_X^2 denote expectation and variance of a random variable X respectively. The index of color channel is omitted for simplicity. This model gives pixel's variance $\sigma_{x_i}^2$ as a linear function of pixel's expectation μ_{x_i} . As discussed in [6, 2], the heteroscedastic noise model characterizes a RAW image more accurately than the conventional AWGN model widely used in image processing. The heteroscedastic noise model in a natural RAW image is illustrated in Figure 1.

In order to study noise statistics in a TIFF image, it is necessary to consider the effects of post-acquisition operations. In this paper, the demosaicing and white-balancing operations are assumed to be linear [10, 12]. Therefore, a short calculation shows that the white-balanced pixel still follows the Gaussian distribution and the relation between its expectation and variance remains linear

$$y_i \sim \mathcal{N}(\mu_{y_i}, \tilde{a}\mu_{y_i} + \tilde{b}), \quad (2)$$

where y_i denotes the white-balanced pixel and the parameters (\tilde{a}, \tilde{b}) differ from the parameters (a, b) due to effects of demosaicing and white-balancing. The white-balanced pixel y_i can be equivalently rewritten as

$$y_i = \mu_{y_i} + \eta_{y_i} \quad \text{with} \quad \eta_{y_i} \sim \mathcal{N}(0, \tilde{a}\mu_{y_i} + \tilde{b}), \quad (3)$$

where η_{y_i} represents the zero-mean signal-dependent noise after white-balancing. Meanwhile, the gamma correction is defined as the following element-wise power-law expression

$$z_i = y_i^{\frac{1}{\gamma}} = (\mu_{y_i} + \eta_{y_i})^{\frac{1}{\gamma}} = \mu_{y_i}^{\frac{1}{\gamma}} \left(1 + \frac{\eta_{y_i}}{\mu_{y_i}}\right)^{\frac{1}{\gamma}}, \quad (4)$$

where γ is the correction factor (typically, $\gamma = 2.2$) and z_i denotes the gamma-corrected pixel. The first order of Taylor's series expansion of $(1+x)^{\frac{1}{\gamma}}$ at $x=0$ leads to

$$z_i = \mu_{y_i}^{\frac{1}{\gamma}} + \frac{1}{\gamma} \mu_{y_i}^{\frac{1}{\gamma}-1} \eta_{y_i} + o\left(\frac{\eta_{y_i}}{\mu_{y_i}}\right) \approx \mu_{z_i} + \frac{1}{\gamma} \mu_{z_i}^{1-\gamma} \eta_{y_i}, \quad (5)$$

where $\mu_{z_i} = \mu_{y_i}^{\frac{1}{\gamma}}$ is the expected value of the gamma-corrected pixel z_i . Taking expectation and variance on the both sides of the equation (5), it follows that

$$\sigma_{z_i}^2 = \frac{1}{\gamma^2} \mu_{z_i}^{2-2\gamma} \sigma_{y_i}^2 = \frac{1}{\gamma^2} \mu_{z_i}^{2-2\gamma} (\tilde{a}\mu_{z_i}^{\gamma} + \tilde{b}). \quad (6)$$

Finally, the gamma-corrected image undergoes the quantization \mathcal{Q}_{Δ} with step Δ in the image acquisition pipeline. Under mild assumptions [13], the quantization noise can be modeled as an additive noise that is uniformly distributed and uncorrelated with the input signal. Taking into account the variance of the quantization noise, the generalized noise model of a natural image is derived as

$$\sigma_{z_i}^2 \triangleq f(\mu_{z_i}; \tilde{a}, \tilde{b}, \gamma) = \frac{1}{\gamma^2} \mu_{z_i}^{2-2\gamma} (\tilde{a}\mu_{z_i}^{\gamma} + \tilde{b}) + \frac{\Delta^2}{12}, \quad (7)$$

where, to simplify the notations, z_i is referred to as the final output pixel. For the sake of simplification, it is assumed that the quantization step is unitary, i.e. $\Delta = 1$. Since this generalized noise model accounts for heteroscedasticity of noise, it is more appropriate to characterize than existing non-linear models used in [8, 7]. The generalized noise model (7) is illustrated in Figure 2.

3. Estimation of Noise Model Parameters from a Single Image

The generalized noise model (7) is non-linear, which causes a difficulty of estimating the noise model parameters. When the gamma factor γ is known in advance, an obvious approach is to invert the gamma correction for obtaining again the heteroscedastic relation (3), and then to perform the Weighted Least Squares (WLS) estimation as proposed in [6]. Unfortunately, this approach leads to many problems in practice [14]. Firstly, the value of γ can not be known in practice. One method is proposed in [15] to estimate γ blindly without calibration information or knowledge of imaging device. However the stability of this method on a large real image database is still questioned. Secondly, even

	TIFF images		JPEG images ($Q = 90$)		JPEG images ($Q = 80$)		JPEG images ($Q = 70$)	
	Avg	Std Dev	Avg	Std Dev	Avg	Std Dev	Avg	Std Dev
$\tilde{a} = -0.0012$	-0.0012	$2.2e^{-4}$	-0.0012	$2.5e^{-4}$	-0.0013	$2.8e^{-4}$	-0.00095	$4.1e^{-4}$
$\tilde{b} = 0.11$	0.114	0.0097	0.117	0.0102	0.126	0.015	0.132	0.025
$\gamma = 0.8$	0.807	0.053	0.811	0.057	0.79	0.058	0.814	0.11
$\tilde{a} = -0.0025$	-0.0024	$3.5e^{-4}$	-0.0024	$4.2e^{-4}$	-0.0026	$5.4e^{-4}$	-0.0023	$5.8e^{-4}$
$\tilde{b} = 0.20$	0.196	0.0084	0.191	0.0098	0.215	0.0117	0.191	0.021
$\gamma = 0.85$	0.845	0.049	0.853	0.058	0.845	0.061	0.842	0.086

Table 1: Parameter estimation on synthetic images

when the value of γ is exactly known, the effect of the quantization Q_Δ makes the inversion of the gamma correction ill-conditioned. Finally, this non-linear inversion would introduce artefacts into the signal, which prevents from obtaining a subsequent good estimation of parameters. Therefore, the goal of this section is to develop an algorithm that works directly on the non-linear generalized noise model (7) for estimating the noise model parameters.

This section presents an algorithm for estimation of noise model parameters from a single image. The proposed algorithm consists of three fundamental steps: homogeneous block detection, level-set segmentation, and Maximum Likelihood (ML) estimation of parameters. The first two steps aim at detecting homogeneous blocks and partition the image into non-overlapping level sets (or segments) in which the pixels are assumed to be independent and identically distributed. Thus local expectations and local variances in each segment can be calculated, allowing to estimate the noise model parameters simultaneously.

3.1. Homogeneous Block Detection and Level-Set Segmentation

Let \mathbf{Z} be a two-dimensional matrix representing a natural image. Firstly, an estimation of image structure is performed using a denoising filter \mathcal{D} : $\mathbf{Z}^{\text{app}} = \mathcal{D}(\mathbf{Z})$ where \mathbf{Z}^{app} denotes the approximate image structure. The residual image \mathbf{Z}^{res} , which is the difference between the noisy image \mathbf{Z} and the denoised image \mathbf{Z}^{app} , is further used to estimate local noise variances. Since it is desirable that the proposed algorithm can be further applied on JPEG images, and JPEG compression works separately on each 8×8 block, it is proposed to decompose the image \mathbf{Z} (accordingly \mathbf{Z}^{app} and \mathbf{Z}^{res}) into 64 vectors of pixels $\mathbf{z}_L = (z_{L,1}, \dots, z_{L,N_b})$, where $L \in \{1, \dots, 64\}$ denotes the location index in the 8×8 grid and N_b is the number of blocks. Therefore, the vector \mathbf{z}_L contains all the pixels at the same location of the 8×8 grid and the pixels $(z_{1,B}, \dots, z_{64,B})$ are in the same block B .

In order to identify if a 8×8 block is homogeneous or contains an edge or discontinuity, it is proposed to calculate the standard deviation of each block and compare it with a threshold τ . The median of absolute deviations (MAD), which is considered as a robust estimator of standard deviation [16], is employed to calculate the standard deviation

of the block. Therefore, the standard deviation of block B is calculated in the DCT domain as follows

$$\hat{\sigma}_B = 1.4826 \cdot \text{MAD}(\text{DCT}(z_{1,B}^{\text{app}}, \dots, z_{64,B}^{\text{app}})). \quad (8)$$

Here, the denoised image \mathbf{Z}^{app} is employed instead of the noisy image \mathbf{Z} because the noise may severely contaminate the calculation of standard deviation. Moreover, only 63 AC coefficients are used in (8). The DC coefficient is excluded. The block B is selected if the standard deviation $\hat{\sigma}_B$ is smaller than the threshold τ . Hence the set of homogeneous blocks is defined by

$$\mathcal{S} = \{1 \leq B \leq N_b : \hat{\sigma}_B \leq \tau\}. \quad (9)$$

After detecting homogeneous blocks, it is proposed to use only a sub-image \mathbf{z}_L for partitioning into K non-overlapping segments by dividing the dynamic range. Each segment S_k , $k \in \{1, \dots, K\}$ is defined by

$$S_k = \{z_{L,B} : z_{L,B}^{\text{app}} \in [u_k - \frac{\Delta_k}{2}, u_k + \frac{\Delta_k}{2}], B \in \mathcal{S}\}. \quad (10)$$

The number of segments K is set to the number of quantization levels, e.g. $K = 2^8$ and $\Delta_k = 1$. If the value of K is larger than the number of quantization levels, the result is finer, i.e. the pixels in each level can be more probably identically distributed, but the number of pixels is smaller, which could lead to a case that there is not enough data for the subsequent parameter estimation. The situation is opposite when the value of K is smaller than the number of quantization levels. For the sake of clarity, the pixel in each segment S_k is now denoted $z_{k,i}$, $i \in \{1, \dots, n_k\}$ where n_k is the number of pixels in segment S_k . Analogously, $z_{k,i}^{\text{app}}$ and $z_{k,i}^{\text{res}}$ denote respectively its denoised value and residual value.

3.2. Maximum Likelihood Estimation

Consequently, local expectation and local variance in each segment are given by

$$\hat{\mu}_k = \frac{1}{n_k} \sum_{i=1}^{n_k} z_{k,i}^{\text{app}} \quad (11)$$

$$\hat{\sigma}_k^2 = \frac{1}{n_k - 1} \sum_{i=1}^{n_k} (z_{k,i}^{\text{res}} - \bar{z}_k^{\text{res}})^2 \quad \text{with} \quad \bar{z}_k^{\text{res}} = \frac{1}{n_k} \sum_{i=1}^{n_k} z_{k,i}^{\text{res}}. \quad (12)$$

Because the local expectation $\hat{\mu}_k$ is calculated as the average of all denoised value in each segment, it is assumed that its variance is negligible when the number of pixels is large, i.e. the local expectation $\hat{\mu}_k$ is close to the true value μ_k : $\hat{\mu}_k \cong \mu_k$. Meanwhile, the variance of $\hat{\sigma}_k^2$ is more crucial and needs to be treated carefully. In virtue of Lindeberg Central Limit Theorem (CLT) [17, theorem 11.2.5], for a very large number of pixels n_k , the local variance $\hat{\sigma}_k^2$ follows the Gaussian distribution

$$\hat{\sigma}_k^2 \sim \mathcal{N}(\sigma_k^2, d_k \sigma_k^4) \quad \text{with} \quad d_k = \frac{2}{n_k}, \quad (13)$$

where $\sigma_k^2 = f(\mu_k; \tilde{a}, \tilde{b}, \gamma)$ is the true variance with respect to μ_k . The Figure 2 illustrates the scatter-plot of couples $\{\hat{\mu}_k, \hat{\sigma}_k^2\}_{k=1}^K$ and the generalized noise model (7) in natural images in JPEG format acquired by *Nikon D70* and *Nikon D200* cameras [9].

The ML approach is used to fit the global parametric model $\sigma_k^2 = f(\mu_k; \tilde{a}, \tilde{b}, \gamma)$ to the scatter-plot of couples $\{\hat{\mu}_k, \hat{\sigma}_k^2\}_{k=1}^K$. The log-likelihood function of K segments is given by

$$\mathcal{L} = -\frac{1}{2} \sum_{k=1}^K \left[\log(2\pi d_k f^2(\hat{\mu}_k; \tilde{a}, \tilde{b}, \gamma)) + \frac{\hat{\sigma}_k^2 - f(\hat{\mu}_k; \tilde{a}, \tilde{b}, \gamma)}{d_k f^2(\hat{\mu}_k; \tilde{a}, \tilde{b}, \gamma)} \right]. \quad (14)$$

Here, because the true value μ_k is unknown in practice, μ_k is replaced by $\hat{\mu}_k$ in the log-likelihood function \mathcal{L} . The ML estimates of $(\tilde{a}, \tilde{b}, \gamma)$ are obtained by maximizing the log-likelihood function \mathcal{L}

$$(\hat{\tilde{a}}, \hat{\tilde{b}}, \hat{\gamma}) = \arg \max_{(\tilde{a}, \tilde{b}, \gamma)} \mathcal{L}(\tilde{a}, \tilde{b}, \gamma). \quad (15)$$

Because there is no closed form for ML estimates, the problem (15) is proposed to be solved numerically by using the Nelder-Mead method [18].

4. Numerical Results

It can be noted that the accuracy of the homogeneous block detection and segmentation depends on the performance of the denoising filter \mathcal{D} . We have conducted some denoising methods such as Gaussian filter, Wiener filter, wavelet-based filter [19] and Block-Matching and 3D (BM3D) filter [20]. The usual denoising methods as Gaussian filter and Wiener filter provide very poor results. The results provided by the wavelet-based filter and BM3D filter are equivalent but the BM3D filter takes much processing time. The wavelet-based denoising filter is employed in this paper because of its relative accuracy and computational efficiency.

The proposed algorithm for estimation of noise model parameters requires an appropriate threshold τ such that we have sufficient statistics for estimation process. In this paper, the threshold τ is defined as the median of absolute deviations of all residual pixels z_i^{res}

$$\tau = 1.4826 \cdot \text{MAD}(z_1^{\text{res}}, \dots, z_N^{\text{res}}). \quad (16)$$

This threshold is simple and efficient for rejecting blocks with strong edges. Besides, the sub-image used segmentation and parameter estimation corresponds to the location (4, 4) of the 8×8 grid since compression error is higher for pixels near block boundaries, and especially high at block corners [21].

4.1. Parameter Estimation on Synthetic Images

The reference images from TID2008 database [22] are chosen to evaluate the accuracy of the proposed approach. The parameters $(\tilde{a}, \tilde{b}, \gamma)$ are used to generate synthetic images according to the generalized noise model (7). Those parameters are estimated from natural JPEG images that are acquired by *Nikon D70* and *Nikon D200* cameras (see Figure 2). The synthetic images are then compressed with different quality factors {70, 80, 90}. The Table 1 shows the statistics of estimated parameters on non-compressed TIFF images and JPEG images with different quality factors. It can be noted that the estimated parameters are close to the ground truth. Moreover, the distortion caused by JPEG compression with moderate-to-high quality factors ($Q \geq 70$) seems to weakly interfere in the estimation process.

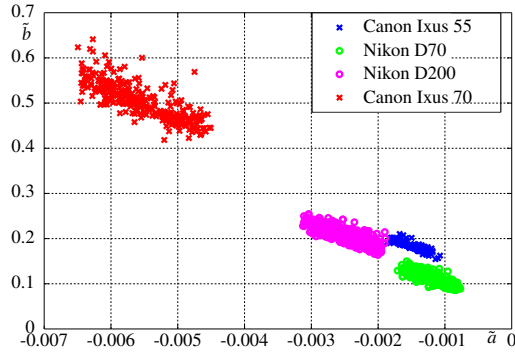


Figure 3: Estimated parameters (\tilde{a}, \tilde{b}) on JPEG images issued from different camera models in Dresden image database [9].

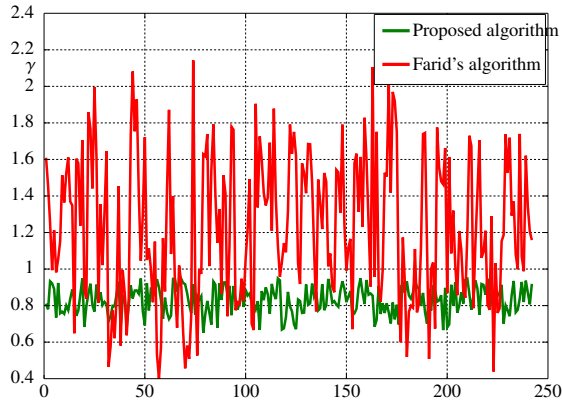


Figure 4: Comparison between the proposed algorithm and Farid's [15] for estimation of gamma factor on JPEG images issued from *Nikon D200* camera model.

Since the generalized noise model (7) has not been proposed yet in the literature, there is no existing algorithm for noise parameter estimation to compare with the proposed one.

4.2. Parameter Estimation on Natural Images

To highlight the relevance of the proposed approach, experiments are then conducted on a large image database. The Dresden database [9] that covers different camera devices, different imaged scenes, different camera settings and different environmental conditions is chosen for this experiment. All images of the database are acquired with the highest available JPEG quality setting and maximum available resolution. Figure 3 shows estimated parameters (\tilde{a}, \tilde{b}) over 1000 JPEG images of different camera models. As expected, the estimated parameters of the same camera model are close to each other. Furthermore, it is desirable to compare estimated gamma provided by the proposed algorithm with the algorithm proposed by Farid [15]. Figure 4 shows estimated gamma of the two algorithms on the JPEG images taken from *Nikon D200* camera model. It can be noted that the variability of gamma estimated by the proposed algorithm is considerably smaller than Farid's, thus the amount of gamma can be estimated more efficiently.

4.3. Application to Image Denoising

To highlight the usefulness of the generalized noise model (7), it is proposed to combine it with the LLMMSE filter [3] to design an efficient image denoising method. The LLMMSE filter is based on the non-stationary mean, non-stationary variance image model. From (5), the pixel z can be decomposed as

$$z = u + \frac{1}{\gamma} u^{1-\gamma} \eta_u, \quad (17)$$

where u denotes the original pixel and η_u is the zero-mean signal-dependent noise, $\sigma_{\eta_u}^2 = \tilde{a}\mu_u^\gamma + \tilde{b}$. The index of pixel is omitted for the sake of clarity. The original pixel u involves non-stationary mean and non-stationary variance. The non-stationary mean describes the gross structure of an image and the non-stationary variance characterizes edge information of the image [3]. In the decomposition (17), the quantization noise is assumed to be negligible. As explained in [3], the LLMMSE filter for any signal-dependent noise model is formulated as

$$\hat{u} = \left(1 - \frac{\sigma_z^2}{\sigma_u^2}\right) \mu_z + \frac{\sigma_z^2}{\sigma_z^2} z, \quad (18)$$

where μ_z and σ_z^2 are respectively local mean and local variance of the pixel z , μ_u and σ_u^2 are respectively local mean and local variance of the original pixel u . Since the noise η_u is zero-mean, it follows from (17) that $\mu_z = \mu_u$. The LLMMSE filter (18) is the weighted sum of original signal mean μ_u and the noisy observation z where the weight is determined as the ratio of the original signal variance and noise variance. A simple technique to obtain local statistics μ_z and σ_z^2 is to calculate over a sliding window of size $(2r+1) \times (2c+1)$

$$\mu_z(m, n) = \frac{1}{(2r+1)(2c+1)} \sum_{i=m-r}^{m+r} \sum_{j=n-c}^{n+c} z(i, j), \quad (19)$$

$$\sigma_z^2(m, n) = \frac{1}{(2r+1)(2c+1)} \sum_{i=m-r}^{m+r} \sum_{j=n-c}^{n+c} (z(i, j) - \mu_z(m, n))^2. \quad (20)$$

Therefore, it remains to calculate the variance σ_u^2 . From (17), the variance σ_z^2 can be given by

$$\sigma_z^2 = \sigma_u^2 + \frac{1}{\gamma^2} \mathbb{E}[u^{2-2\gamma}] \sigma_{\eta_u}^2. \quad (21)$$

By using the Taylor series expansion of $u^{2-2\gamma}$ around μ_u , the expression of $\mathbb{E}[u^{2-2\gamma}]$ can be simplified as

$$\mathbb{E}[u^{2-2\gamma}] = \mu_u^{2-2\gamma} + (1-\gamma)(1-2\gamma)\mu_u^{-2\gamma}\sigma_u^2. \quad (22)$$

Combining (21) and (22), the expression of the variance σ_u^2 is derived as

$$\sigma_u^2 = \frac{\sigma_z^2 - \frac{1}{\gamma^2} \mu_u^{2-2\gamma} \sigma_{\eta_u}^2}{1 + \frac{1}{\gamma^2} (1-\gamma)(1-2\gamma) \mu_u^{-2\gamma} \sigma_{\eta_u}^2}. \quad (23)$$

The LLMSSE filter (18) follows immediately.

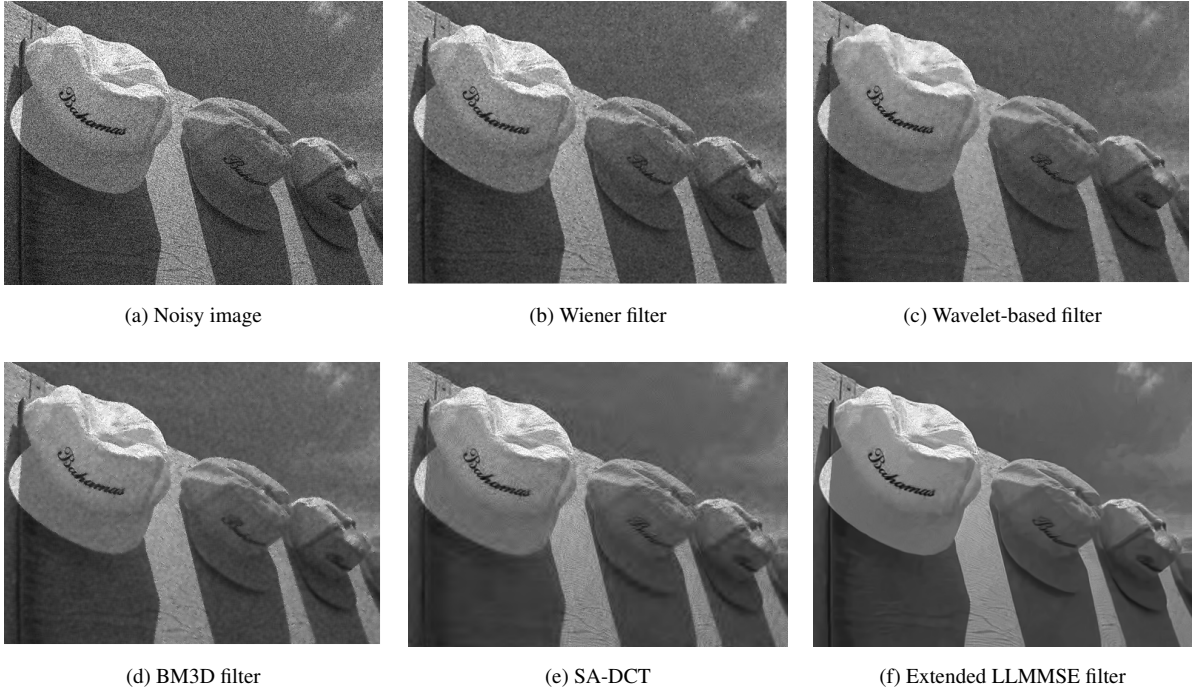


Figure 5: Illustration of different denoising filters for $\tilde{a} = 1$, $\tilde{b} = 10$, $\gamma = 0.85$.

To evaluate the denoising performance of the extended LMMSE filter, experiments are conducted on the synthetic non-compressed images generated from TID2008 database. The parameters $(\tilde{a}, \tilde{b}, \gamma)$ are estimated on each synthetic image. Estimated parameters are then used in the extended LMMSE filter. Table 2 shows the averaged Peak Signal-to-Noise Ratio (PSNR) of the extended LMMSE filter compared with other denoising methods, e.g. some classical methods such as Wiener filter and wavelet-based filter [19], and some state-of-the-art methods such as BM3D filter [20] and Shape-Adaptive DCT (SA-DCT) filter [23]. It can be noted that the extended LMMSE filter outperforms the Wiener, wavelet-based, BM3D, and is rather equivalent to the SA-DCT filter. This can be justified due to the fact that the SA-DCT is designed for signal-dependent noise whilst the others do not consider the non-stationarity of noise. Different denoising filters are illustrated in Figure 5.

Remark 1. *One of the main contributions of the paper is to propose the generalized noise model that has not been provided yet in the literature. This work is accomplished by studying the main steps of the image processing pipeline inside a digital camera. The relevance of the proposed model is highlighted by applying on a real image database. However, this approach involves a limitation, namely that the demosaicing and white balancing are not completely modeled. The proposed approach assumes that those operations are linear, which simplifies the statistical study and results in a more exploitable model, say the generalized noise model. It must be noted that the demosaicing always involves a convolution operation, which requires us to consider multivariate distribution. The resulting model could be more relevant but inexploitable in practice. Overall, the generalized noise model can be seen as a trade-off between*

	Simple Wiener filter	Wavelet-based filter [19]	BM3D filter [20]	SA-DCT filter [23]	Extended LLMMSE filter
$\tilde{a} = -0.0012$ $\tilde{b} = 0.11$ $\gamma = 0.8$	30.06	41.33	42.85	49.75	50.97
$\tilde{a} = -0.0025$ $\tilde{b} = 0.20$ $\gamma = 0.85$	30.05	40.37	42.56	47.73	48.61
$\tilde{a} = 1$ $\tilde{b} = 10$ $\gamma = 0.85$	24.88	26.13	26.32	27.08	29.14

Table 2: PSNR of different denoising filters

the reality in image acquisition and the exploitability in practice.

5. Conclusion

This paper proposes a novel generalized signal-dependent noise model that is more relevant to characterize a natural image acquired by a digital camera. An algorithm for estimating noise model parameters accurately from a single image is also designed. The proposed algorithm can work on JPEG images with moderate-to-high quality factors. Another strength of the proposed algorithm is the ability to estimate the gamma factor more efficiently. Moreover, the LLMMSE filter is extended by combining with the proposed generalized noise model. The proposed noise model could be useful in many applications. A first step is to exploit the parameters of the generalized noise model as camera fingerprint for camera model identification, as proposed in [24].

References

- [1] G. E. Healey, R. Kondepudy, Radiometric CCD camera calibration and noise estimation, *IEEE Trans. Pattern Anal. Mach. Intell.* 16 (3) (1994) 267–276.
- [2] A. Foi, M. Trimeche, V. Katkovnik, K. Egiazarian, Practical Poissonian-Gaussian noise modeling and fitting for single-image raw-data, *IEEE Trans. Image Process.* 17 (10) (2008) 1737–1754.
- [3] D. T. Kuan, A. A. Sawchuk, T. C. Strand, P. Chavel, Adaptive noise smoothing filter for images with signal-dependent noise, *IEEE Trans. Pattern Anal. Mach. Intell.* 7 (2) (1985) 165–177.
- [4] F. Luisier, T. Blu, M. Unser, Image denoising in mixed Poisson-Gaussian noise, *IEEE Trans. Image Process.* 20 (3) (2011) 696–708.
- [5] M. Makitalo, A. Foi, Optimal inversion of the generalized Anscombe transformation for Poisson-Gaussian noise, *IEEE Trans. Image Process.* 22 (1) (2013) 91–103.
- [6] T. H. Thai, R. Cogranne, F. Reiraint, Camera model identification based on the heteroscedastic noise model, *IEEE Trans. Image Process.* 23 (1) (2014) 250–263.
- [7] H. Faraji, W. J. MacLean, CCD noise removal in digital images, *IEEE Trans. Image Process.* 15 (9) (2006) 2676–2685.
- [8] X. Liu, M. Tanaka, M. Tokunomi, Estimation of signal dependent noise parameters from a single image, in: *Proc. IEEE Int. Conf. Image Process.*, 2013, pp. 79–82.

- [9] T. Gloe, R. Bohme, The Dresden image database for benchmarking digital image forensics, in: Proc. ACM Symposium Applied Comput., Vol. 2, 2010, pp. 1585–1591.
- [10] R. Ramanath, W. E. Snyder, Y. Yoo, M. S. Drew, Color image processing pipeline, *IEEE Signal Process. Mag.* 22 (1) (2005) 34–43.
- [11] T. H. Thai, R. Cogranne, F. Retraint, Statistical model of natural images, in: Proc. IEEE. Int. Conf. Image Process., 2012, pp. 2525–2528.
- [12] T. H. Thai, R. Cogranne, F. Retraint, Statistical model of quantized DCT coefficients: Application in the steganalysis of Jsteg algorithm, *IEEE Trans. Image Process.* 23 (5) (2014) 1980–1993.
- [13] B. Widrow, I. Kollar, M.-C. Liu, Statistical theory of quantization, *IEEE Trans. Instrum. Meas.* 45 (2) (1996) 353–361.
- [14] R. P. Kleihorst, R. L. Lagendiik, J. Biemond, An adaptive order-statistic noise filter for gamma-corrected image sequences, *IEEE Trans. Image Process.* 6 (10) (1997) 1442–1446.
- [15] H. Farid, Blind inverse gamma correction, *IEEE Trans. Image Process.* 10 (10) (2001) 1428–1433.
- [16] P. J. Rousseeuw, C. Croux, Alternatives to the median absolute deviation, *J. Amer. Statist. Assoc.* 88 (424) (1993) 1273–1283.
- [17] E. L. Lehmann, J. P. Romano, *Testing Statistical Hypotheses*, 3rd Edition, Springer, New York, 2005.
- [18] J. A. Nelder, R. Mead, A simplex method for function minimization, *Comput. J.* 7 (1965) 308–313.
- [19] M. K. Mihçak, I. Kozintsev, K. Ramchandran, Spatially adaptive statistical modeling of wavelet image coefficients and its application to denoising, in: Proc. IEEE Int. Conf. Acoust., Speech, Signal Process., Vol. 6, 1999, pp. 3253–3256.
- [20] K. Dabov, A. Foi, V. Katkovnik, K. Egiazarian, Image denoising by sparse 3-d transform-domain collaborative filtering, *IEEE Trans. Image Process.* 16 (8) (2007) 2080–2095.
- [21] M. A. Robertson, R. L. Stevenson, DCT quantization noise in compressed images, *IEEE Trans. Circuits Syst. Video Technol.* 15 (1) (2005) 27–38.
- [22] N. Ponomarenko, V. Lukin, A. Zelensky, K. Egiazarian, M. Carli, F. Battisti, TID2008 - a database for evaluation of full-reference visual quality assessment metrics, *Advances Modern Radioelectronics* 10 (2009) 30–45.
- [23] A. Foi, V. Katkovnik, K. Egiazarian, Pointwise shape-adaptive DCT for high-quality denoising and deblocking of grayscale and color images, *IEEE Trans. Image Process.*, 16 (5) (2007) 1395–1411.
- [24] T. H. Thai, F. Retraint, R. Cogranne, Camera model identification based on generalized noise model in natural images, *Signal Processing*, 48 (1), (2016) 285–297.